Accurate remote vital sign monitoring with 10ghz ultra-wide patch antenna array

Rabbani, Muhammad Saqib; Ghafouri-shiraz, Hooshang

DOI:
10.1016/j.aeue.2017.04.024

Document Version
Peer reviewed version

Citation for published version (Harvard):
Rabbani, MS & Ghafouri-shiraz, H 2017, 'Accurate remote vital sign monitoring with 10ghz ultra-wide patch antenna array', *AEU - International Journal of Electronics and Communications*, vol. 77, pp. 36-42. https://doi.org/10.1016/j.aeue.2017.04.024

Accepted Manuscript

Regular paper

Accurate Remote Vital Sign Monitoring with 10GHz Ultra-wide Patch Antenna Array

Muhammad Saqib Rabbani, Hooshang Ghafouri-Shiraz

PII: S1434-8411(17)30177-2
DOI: http://dx.doi.org/10.1016/j.aeue.2017.04.024
Reference: AEUE 51858

To appear in: *International Journal of Electronics and Communications*

Received Date: 24 January 2017
Accepted Date: 21 April 2017

Please cite this article as: M.S. Rabbani, H. Ghafouri-Shiraz, Accurate Remote Vital Sign Monitoring with 10GHz Ultra-wide Patch Antenna Array, *International Journal of Electronics and Communications* (2017), doi: http://dx.doi.org/10.1016/j.aeue.2017.04.024

Accurate Remote Vital Sign Monitoring with 10GHz Ultra-wide Patch Antenna Array

Muhammad Saqib Rabbani[†], Hooshang Ghafouri-Shiraz [*]

School of Electronic Electrical and System Engineering, University of Birmingham,

Edgbaston, B15 2TT, UK

[†]saqibrabbani05@hotmail.com

[*]ghafourh@bham.ac.uk

Abstract: A patch antenna array has been presented at 10GHz frequency with improved gain (14dBi) and far-field radiation capabilities for accurate detection of human respiration and heart beat rate with Doppler radar technique. The measured and simulation antennas' results showed good agreement. Feasibility of 10GHz channel has been studied for remote vital sign monitoring (RVSM) under Doppler radar theory. Both the breathing rate (BR) and heart rate (HR) of a man have been accurately detected from various distances ranging from 5cm to 4m with as small transmitted power as −10dBm.

Keywords: Patch antenna array, Doppler radar, remote vital sign monitoring, Doppler radar theory, 10GHz microstrip antenna

1. Introduction

Remote monitoring of respiration and heart beat rate with Doppler radar is a more convenient way to check the vitality signs of a person as compared to the conventional vital sign monitoring devices which need direct sensors plantation on the subject body [1-5]. RVSM finds its applications in regular and special health care, emergency services, security and defence sectors [1-10].

RVSM with Doppler radar at low power ultra-wide band frequencies (UWB) (3.1GHz-10.6GHz) has become quite popular due to several reasons like low electromagnetic (EM) interference, high EM wave penetration, low power consumption, etc. [11-18]. For such UWB RVSM systems, appropriate antenna design plays a crucial role in both the precision of

the detected vital signs as well as in overall system compactness [14]. Microstrip patch antenna arrays have been widely employed in RVSM systems due to their low profile, low cost, ability to make arrays to attain high gain and small beam-widths [12-19]. In [12], arrays of 2×2 microstrip patch elements are deployed in RVSM at UWB frequencies. The arrays are designed with the conventional method in cooperation with parallel feeding lines and multiple impedance transformation networks. The reported gain in [12] is 9dBi at 5GHz however practically achievable maximum gain with conventional microstrip antenna array of 2×2 patch elements at UWB frequencies is around 12dBi [20]. Moreover, the reported patch arrays are quite bulky in size which may abstain to integrate them with modern real life compact and portable devices including smartphones and tablets.

In this paper, an ultra-wide patch antenna array design has been deployed for accurate detection of human BR and HR at 10GHz frequency. The ultra-wide patch elements provided a good trade-off between the arrays gain and size. Feasibility of 10GHz frequency for RVSM has been presented under the Doppler radar principle. Both the BR and HR have been simultaneously measured of the subject sitting in front of the antennas and having continuous normal breathing. The low side lob levels, high gains and adequate beam-widths of the designed array confined the EM wave on the subject chest which ultimately improved the accuracy of measured RVSM. This paper is organized as follows: Section 2 describes the antenna design procedure, section 3 presents the antenna results, section 4 shows the feasibility of 10GHz frequency for RVSM, Section 5 demonstrates the measured RVSM results and section 5 concludes the work.

2. Antenna Design and Results

A microstrip patch antenna array has been designed for X-band frequencies centered at 10GHz on low loss RT/Duroid 5880 substrate with thickness 'h'=1.57mm, dielectric constant $\varepsilon_r = 2.2$ and copper cladding 't'=35μm as explained in [21-23]. The structure

diagram of the antenna array is presented in Fig. 1. The array is comprised of only two symmetrical ultra-wide patch elements which are fed in series.

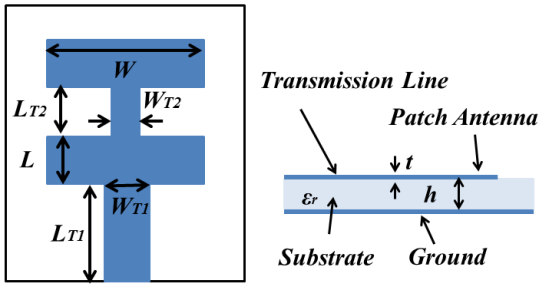

(a) (b)

Fig. 1. Structure of the designed antenna array. (a) Front view and (b) Side view

Two copies of the microstrip patch antenna arrays, one for transmitter and the other for receiver, have been fabricated with the proposed method as described in the last section. Fig. 2 demonstrates the fabricated antennas and Table 1 shows their dimensions.

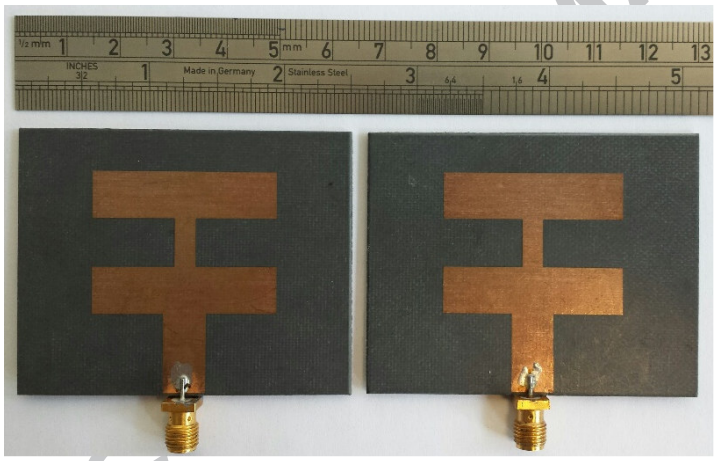

(a) (b)

Fig. 2. Two copies of the fabricated antennas. (a) Transmitter's antenna and (b) receiver's antenna

L	W	L_{T1}	L_{T2}	W_{T1}	W_{T2}
9.03	34.35	15.39	9.03	8.1	4.05

Table 1 Dimensions (mm) of the fabricated antennas

Fig. 3(a) shows the simulation and measured return loss (S_{11}) and gain responses of the fabricated antennas. It is clear from Fig. 3 that both of the fabricated antennas show almost similar S_{11} response with -10dB bandwidth of around 1.28GHz and gain of 13.9dBi at 10GHz. It can also be noticed that at 10GHz the S_{11} of antennas 2(a) and (b) are better than -13dB and -15.7 dB, respectively. Figs. 3(b) and (c) present the measured and simulation far-field patterns (FFP) of the antennas shown in Figs. 2(a) and (b), respectively, in both E and H planes at 10GHz frequency. It is obvious from Figs. 4 and 5 that the antennas' main lobs are directed to about 0 degree in both E and H planes for all the cases and the side lob levels are at most below -13dB. The half power beam-widths are about 320 and 350 in H and E planes, respectively. This way, it is calculated that for a subject's chest width of 30cm the antenna radiation beam is confined on the chest when the antenna is placed up to a distance of around 50cm. Therefore, it is expected that an antenna distance of around 50cm may be the best choice for RVSM with the proposed antenna system.

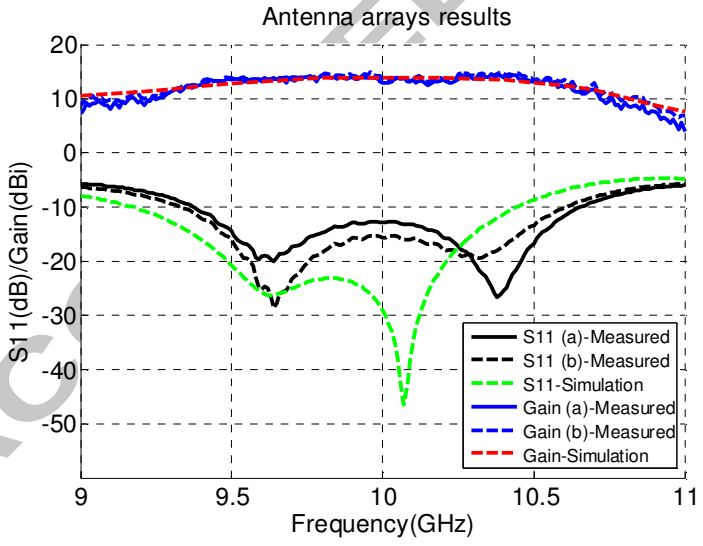

(a)

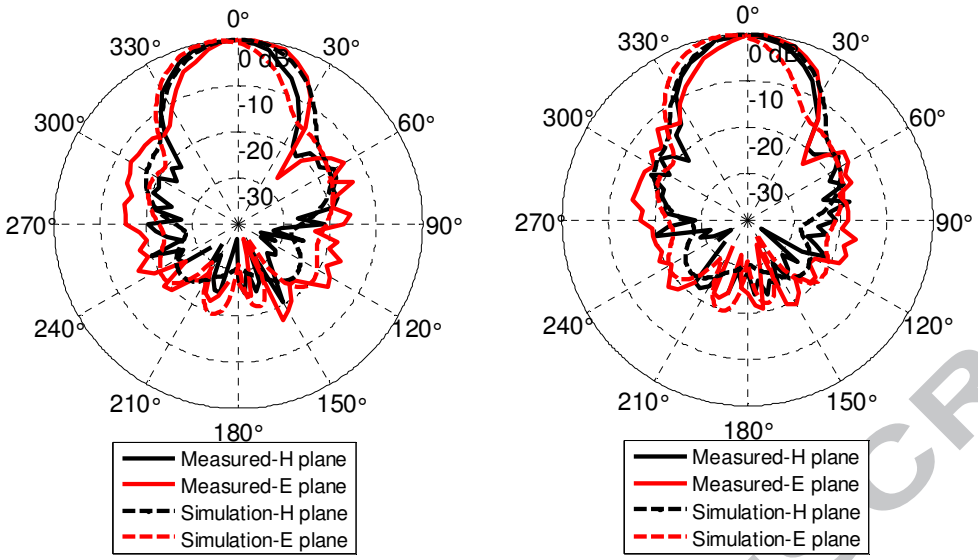

(b) (c)

Fig. 3. Antennas results. (a) S_{11} and gain of antennas shown in Figs. 2(a) and (b) and FFP in E and H planes at 10GHz of antennas shown in (b) Fig. 2(a), and (c) Fig. 2(b)

3. RVSM with 10GHz Doppler Radar

According to the Doppler radar theory employed for RVSM, the transmitted (*Tx*) signal $S(t) = \cos(2\pi ft + \phi(t))$, where f and $\phi(t)$ are the frequency and phase noise of the transmitted wave, respectively, is phase modulated with BR and HR signals when it is reflected back from the subject body. The received base band signal *R(t)* may be approximated as [24]:

$$R(t) = \cos\left[\theta(t) + \frac{4\pi x_b(t)}{\lambda_0} + \frac{4\pi x_h(t)}{\lambda_0}\right] \qquad (1)$$

where $\theta(t)$ is the total phase shift due to the signal path, reflections from the subject and surroundings and residual phase noise. $x_b(t)$ and $x_h(t)$ are chest vibration displacements due to respiration and heartbeat, respectively. The displacements $x_b(t)$ and $x_h(t)$ may be approximated as: $x_b(t) = m_b \sin(2\pi f_b t)$ and $x_h(t) = m_h \sin(2\pi f_h t)$, where m_b and m_h are the

displacement amplitudes of the chest motion due to respiration and heartbeat, respectively. f_b and f_h are the frequencies of BR and HR, respectively [24]. Ultimately, expanding eq. (1) in Fourier series and taking the first positive harmonics of both f_b and f_h into account may leads to: [25]:

$$R(t) = J_1\left[\frac{4\pi m_b}{\lambda_0}\right] J_0\left[\frac{4\pi m_h}{\lambda_0}\right] \cos(2\pi f_b t + \theta) + J_0\left[\frac{4\pi m_b}{\lambda_0}\right] J_1\left[\frac{4\pi m_h}{\lambda_0}\right] \cos(2\pi f_h t + \theta) \quad (2)$$

where $J_n(X)$ is Bessel function of first kind with argument X.

The coefficients $J_1\left[\frac{4\pi m_b}{\lambda_0}\right] J_0\left[\frac{4\pi m_h}{\lambda_0}\right]$ and $J_0\left[\frac{4\pi m_b}{\lambda_0}\right] J_1\left[\frac{4\pi m_h}{\lambda_0}\right]$ are the amplitudes of the phase variations in $R(t)$ due to respiration and heartbeat, respectively [25]. It may worth to mention that although about the forth harmonic of the BR signal comes in the range of HR signal but it is assumed to be insignificant due to its negligibly small amplitude compared to the HR signal amplitude [18]. For our current case of RVSM at 10GHz frequency λ_0=30mm and m_b and m_h are in the ranges of $(8-12)mm$ and $(0.2-0.5)mm$, respectively, for a person at rest with normal breathing [26]. Equation (6) is visualized in Fig. 4 which shows the phase amplitude variations of $R(t)$ signal for various combinations of m_b and m_h at λ_0=30mm with (a) BR and HR in combined, (b) only BR and (c) only HR. From Fig. 4(a) it can be seen that the maximum $R(t)$ amplitude goes up to around 108^0 which is suitably high for RVSM detection as well as it is small enough to stay linear within -180^0 to $+180^0$ of phase shift range. Fig. 4(b) indicates that BR signal does not suffer with any null detection (0 value) for the given m_b and m_h combinations and always remain obvious in the detected signal. On the other hand, Fig. 4(c) shows that the phase variation in the received signal due to HR is only a few degrees which is much smaller than that due to BR. It can be predicted from Fig. 4(c)

that the HR signal may suffer with fading for high chest displacement of around 11.5mm with BR. However, it is clear that the likelihood of HR detection is much higher than its null detection across the chest displacement range of 8-12mm for average people. Furthermore, it is obvious from eq. (2) and Fig. 4(c) that the radar's tone frequency can be adjusted within the antennas bandwidth (9.4-10.6GHz) to shift the null detection point away when it is caused by the mentioned combinations of the BR and HR amplitudes. Nevertheless, the noise in θ (see eq. (2)) due to the surrounding reflections should be minimized by appropriate designing of narrow beam focusing antennas at *Tx* and *Rx* for accurate detection of HR so that the amplitude variations in *R(t)* mostly originate from the subject chest.

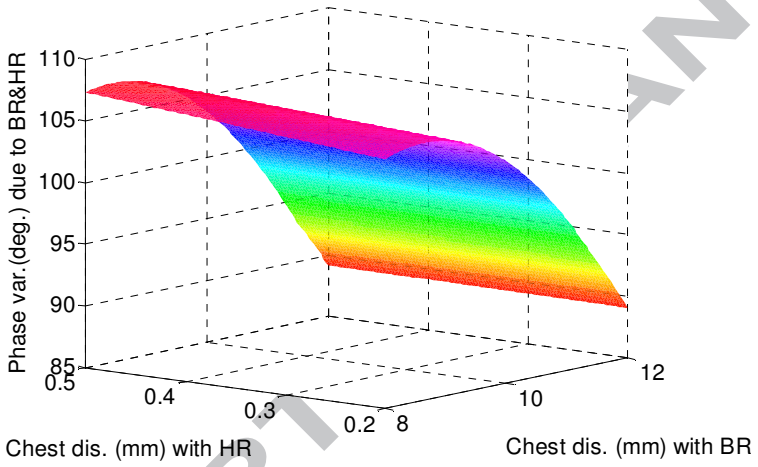

(a)

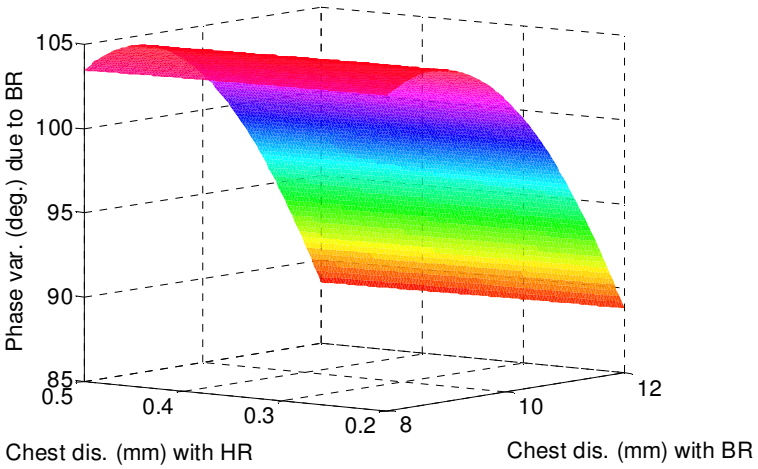

(b)

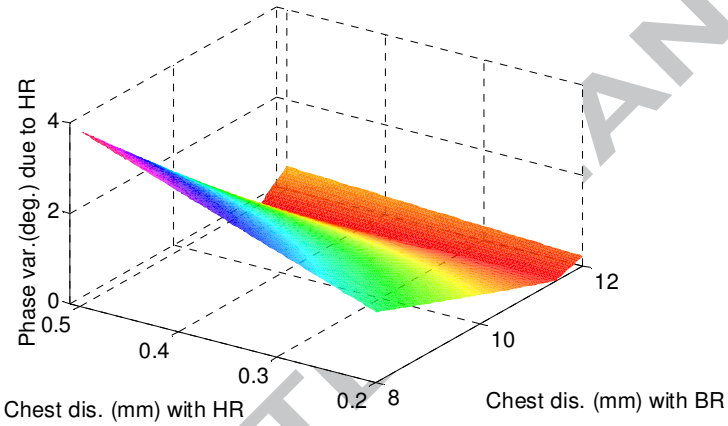

(c)

Fig. 4. Magnitude of the phase amplitude variation of *R(t)* in eq. (2) for various combinations of m_b and m_h due to: (a) Both BR and HR in combined, (b) Just BR signal and (c) Just HR signal

4. RVSM Results and Discussions

Fig. 5(a) shows the block diagram of various stages of RVSM process with Doppler radar. Fig. 5(b) demonstrates the experiment setup to measure the RVSM at 10GHz frequency. Keysight Technology's 20GHz VNA 'N5232A' is used as transmitter and receiver. The

RVSM data is acquired with two ways; (i) with a single antenna employed for both transmission and reception and (ii) with dual antennas one for transmission and the other for reception. A normally breathing person sits in front of the antennas iteratively at various distances (d) and the phase of the correlated received signal (S_{11} for single antenna and S_{21} for double antenna) is recorded for 60 seconds for the each iteration. The recorded data is then processed in Matlab program through various digital signal processing stages and the targeted BR and HR is extracted. The major parts of digital signal processing include digital filtering of the recorded raw data in time domain and Discrete Fast Fourier Transformation of the filtered data.

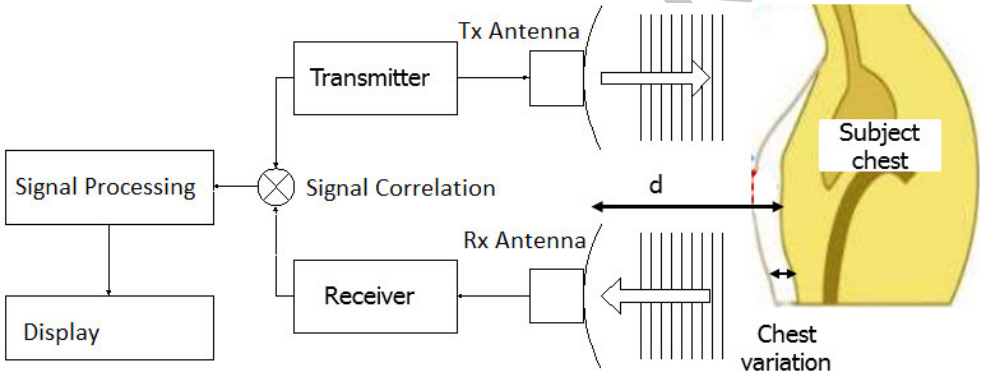

(a)

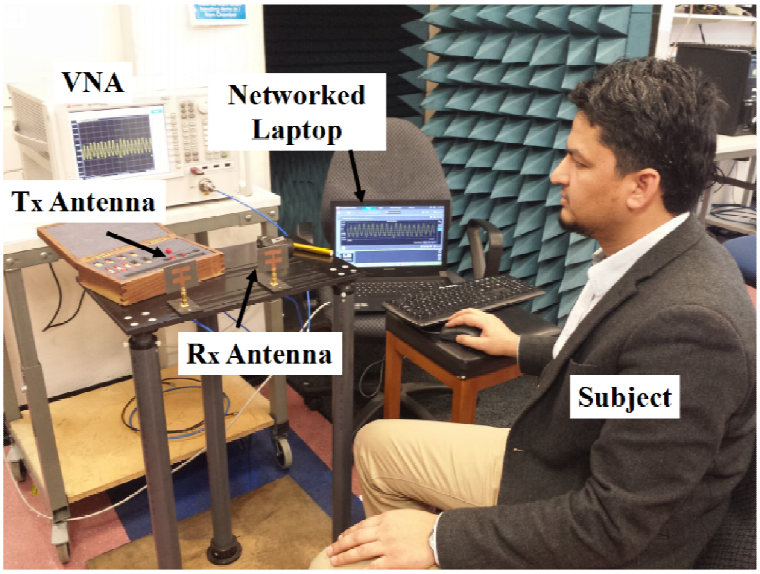

(b)

Fig. 5. RVSM process. (a) Block diagram of various stages of RVSM and (b) experiment setup for RVSM measurements

With the single antenna operations the RVSM experiment is conducted for the subject at 5cm and 54cm distances whereas for the dual antenna operations the experiment is repeated for even longer distances ranging from 24cm to 4m. It can be noticed that the medium distances, where the surrounding phase noise is less effective, are set to be odd multiples of the operating wavelength to keep the received signal's overall phase variation linear within -180 to +180 degrees rage.

Figs. 6 and 7 illustrates the measured RVSM data when the single antenna shown in Fig. 2(a) is employed from 5cm and 54cm distances, respectively, whereas Figs. 8-11 illustrate the measured RVSM data with double antennas shown in Figs. 2(a)-(b) with antennas in (a)-(b) being employed as transmitter and receiver, respectively, at various distances. The sub-figures (a) and (b) in Figs, 6-11 represent the recorded raw data in time domain and processed data in frequency (1/min) domain, respectively. In Figs. 6-11(b)'s, the lower-frequency and high-frequency peaks are expected to be respiration and heartbeat tones, respectively. Both

the BR and HR peaks can be clearly noticed in all the cases in Figs. 6-11(b)'s. All of the detected BR and HR results of RVSM are shown in Table 2 where it clear that in all the cases both the BR and HR results are consistent within their expected ranges [27]. The measured BR and HR in all the cases are also matched to the ones obtained by manual counting using stopwatch. Furthermore, by comparing Figs. 6(b) and 7(b) it is noticed that in case of single antenna operation the HR peak is more obvious when the antenna is placed at very short distance (5cm). On the other hand, it case of dual antennas operation it has been found that the HR peak becomes higher with the longer antenna distance 'd' but it adds more noise to the detected HR peak. Therefore, it can be concluded that with dual antennas operation an antenna distance of around 50cm could be a good choice to detect a clean and rigorous HR signal with the proposed antenna system.

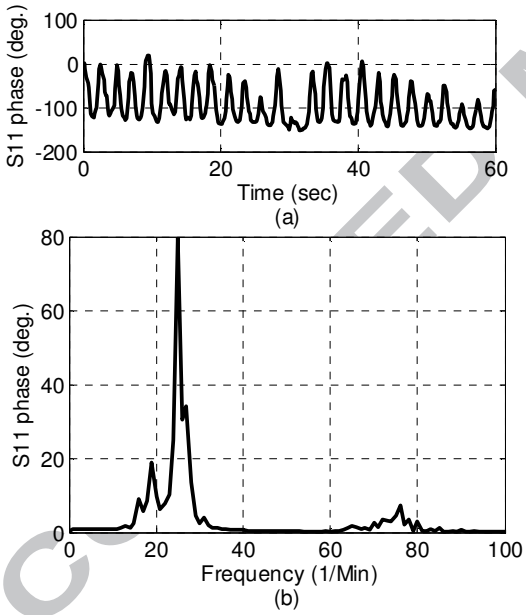

Fig. 6. RVSM measurement from 5cm. (a) Recorded raw data in time domain and (b) detected BR and HR peak

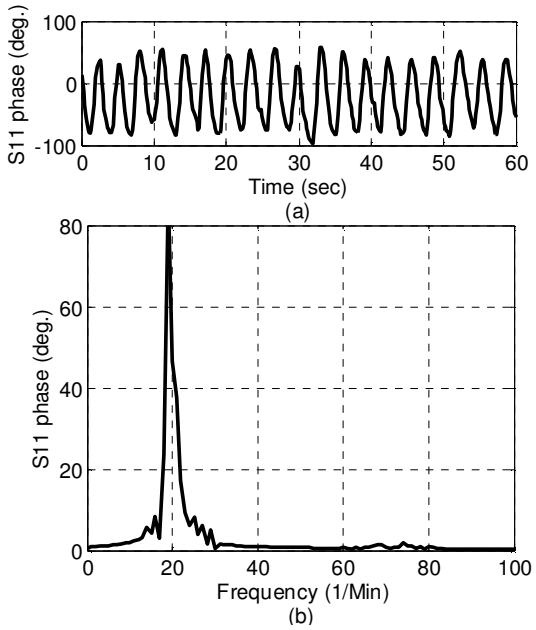

Fig. 7. RVSM measurement from 54cm. (a) Recorded raw data in time domain and (b) detected BR and HR peaks

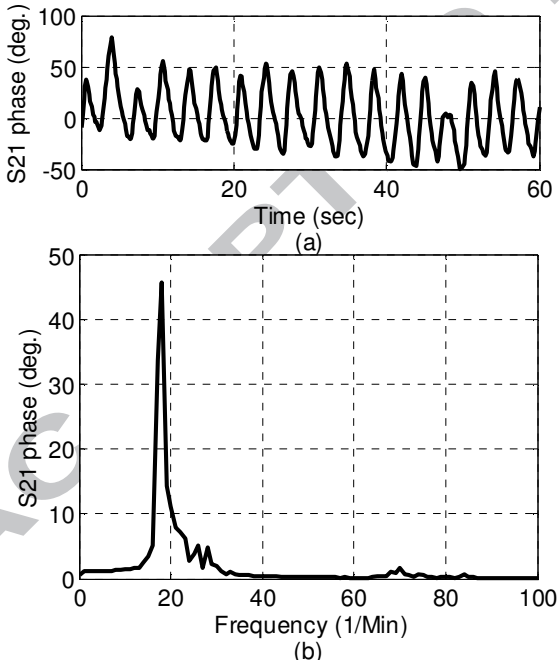

Fig. 8. RVSM measurement from 24cm. (a) Recorded raw data in time domain and (b) detected BR and HR peaks

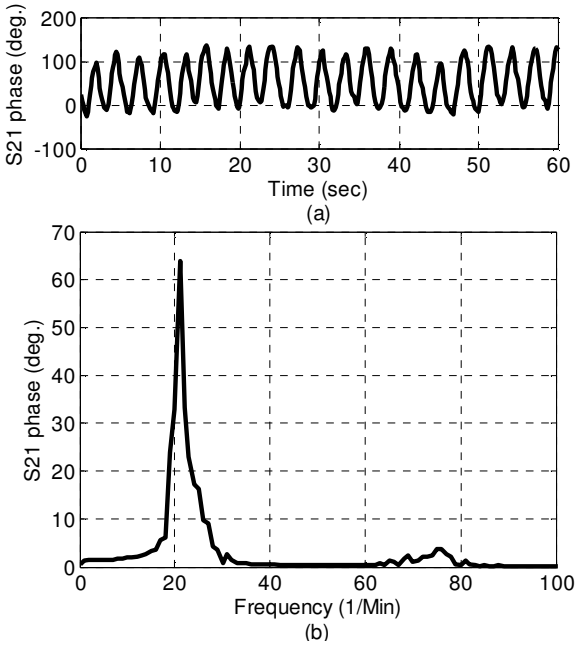

Fig. 9. RVSM measurement from 46cm. (a) Recorded raw data in time domain and (b) detected BR and HR peaks

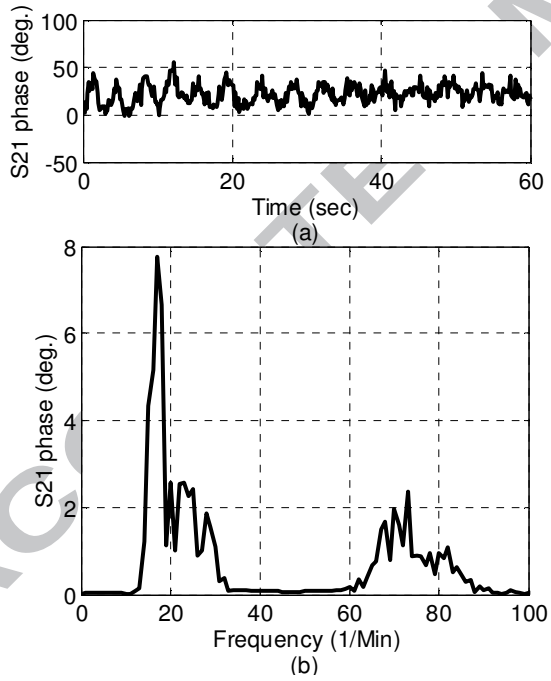

Fig. 10. RVSM measurement from 3m. (a) Recorded raw data in time domain and (b) detected BR and HR peaks

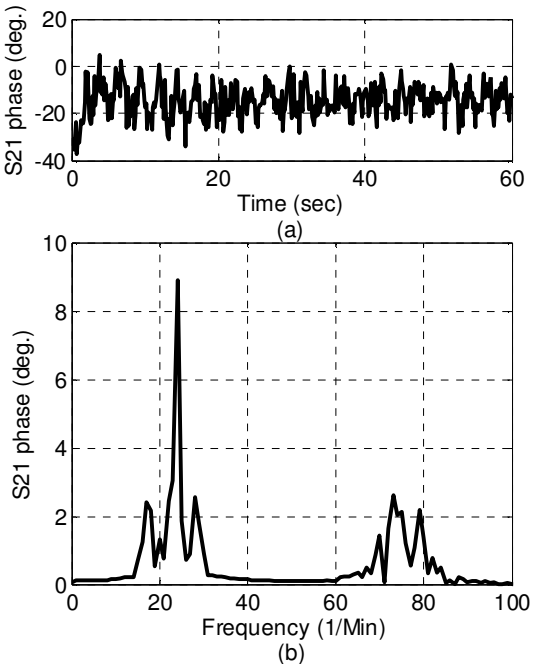

Fig. 11. RVSM measurement from 4m. (a) Recorded raw data in time domain and (b) detected BR and HR peaks

	Single antenna		Dual antennas			
d(cm)	5	54	24	46	300	400
BR	25	19	18	21	17	24
HR	76	74	70	76	73	73

Table 2 Measured BR and HR from various distances

5. Conclusion

Microstrip patch antenna array has been presented for RVSM at 10GHz frequency with UWB Doppler radar. The tested antennas showed good performance in terms of bandwidth, gain and side lob levels for RVSM measurements. Theoretical analysis of RVSM with 10GHz Doppler radar has been presented. The antennas bandwidth (9.4-10.6GHz) gives an extra flexibility to adjust the transmitter's tone frequency to avoid the null detection of HR signal caused by various combinations of the BR and HR amplitudes. Both the BR and HR have been successfully measured with the proposed antennas from various distances ranging from 5cm to 4m within the ordinary lab environment. For the future work, further higher gain and

narrower beam-width antennas may be employed for even longer distance for outdoor RVSM. Moreover, the proposed microstrip antennas can be implemented in other X-band radar applications [28-30].

References:

[1] Sun L, Li Y, Hong H, Xi F, Cai W, Zhu X. Super-resolution spectral estimation in short-time non-contact vital sign measurement. Review of Scientific Instruments. 2015 Apr 1;86(4):044708.

[2] Droitcour AD, Seto TB, Park BK, Yamada S, Vergara A, El Hourani C, Shing T, Yuen A, Lubecke VM, Boric-Lubecke O. Non-contact respiratory rate measurement validation for hospitalized patients. In2009 Annual International Conference of the IEEE Engineering in Medicine and Biology Society 2009 Sep 3 (pp. 4812-4815). IEEE.

[3] Villarroel M, Guazzi A, Jorge J, Davis S, Watkinson P, Green G, Shenvi A, McCormick K, Tarassenko L. Continuous non-contact vital sign monitoring in neonatal intensive care unit. Healthcare technology letters. 2014 Sep;1(3):87.

[4] Suzuki S, Matsui T, Kagawa M, Asao T, Kotani K. An approach to a non-contact vital sign monitoring using dual-frequency microwave radars for elderly care. Journal of Biomedical Science and Engineering. 2013 Jul 8;6(07):704.

[5] Li C, Cummings J, Lam J, Graves E, Wu W. Radar remote monitoring of vital signs. IEEE Microwave Magazine. 2009 Feb;10(1):47-56.

[6] Uenoyama M, Matsui T, Yamada K, Suzuki S, Takase B, Suzuki S, Ishihara M, Kawakami M. Non-contact respiratory monitoring system using a ceiling-attached microwave antenna. Medical and Biological Engineering and Computing. 2006 Sep 1;44(9):835-40.

[7] Ren L, Koo YS, Wang H, Wang Y, Liu Q, Fathy AE. Noncontact Multiple Heartbeats Detection and Subject Localization Using UWB Impulse Doppler Radar. IEEE Microwave and Wireless Components Letters. 2015 Oct;25(10):690-2.

[8] Adib F, Mao H, Kabelac Z, Katabi D, Miller RC. Smart homes that monitor breathing and heart rate. InProceedings of the 33rd Annual ACM Conference on Human Factors in Computing Systems 2015 Apr 18 (pp. 837-846). ACM.

[9] Suzuki S, Matsui T, Kawahara H, Ichiki H, Shimizu J, Kondo Y, Gotoh S, Yura H, Takase B, Ishihara M. A non-contact vital sign monitoring system for ambulances using

dualfrequency microwave radars. Medical & biological engineering & computing. 2009 Jan 1;47(1):101-5.

[10] Bruser C, Antink CH, Wartzek T, Walter M, Leonhardt S. Ambient and Unobtrusive Cardiorespiratory Monitoring Techniques. IEEE reviews in biomedical engineering. 2015;8:30-43.

[11] Tariq A, Ghafouri□Shiraz H. Noncontact heart rate monitoring using Doppler radar and continuous wavelet transform. Microwave and Optical Technology Letters. 2011 Aug 1;53(8):1793-7.

[12] Li C, Xiao Y, Lin J. A 5GHz Double-Sideband Radar Sensor Chip in 0.18 m CMOS for Non-Contact Vital Sign Detection. IEEE Microwave and Wireless Components Letters. 2008 Jul;18(7):494-6.

[13] Li C, Yu X, Lee CM, Li D, Ran L, Lin J. High-sensitivity software-configurable 5.8GHz radar sensor receiver chip in 0.13-m CMOS for noncontact vital sign detection. IEEE Transactions on Microwave Theory and Techniques. 2010 May;58(5):1410-9.

[14] Li C, Xiao Y, Lin J. Design guidelines for radio frequency non-contact vital sign detection. In2007 29th Annual International Conference of the IEEE Engineering in Medicine and Biology Society 2007 Aug 22 (pp. 1651-1654). IEEE.

[15] Li C, Lin J. Complex signal demodulation and random body movement cancellation techniques for non-contact vital sign detection. InMicrowave Symposium Digest, 2008 IEEE MTT-S International 2008 Jun 15 (pp. 567-570). IEEE.

[16] Li C, Ling J, Li J, Lin J. Accurate Doppler radar noncontact vital sign detection using the RELAX algorithm. IEEE Transactions on Instrumentation and Measurement. 2010 Mar;59(3):687-95.

[17] Gu C, Li C, Lin J, Long J, Huangfu J, Ran L. Instrument-based noncontact Doppler radar vital sign detection system using heterodyne digital quadrature demodulation architecture. IEEE Transactions on Instrumentation and Measurement. 2010 Jun;59(6):15808.

[18] Li C, Lubecke VM, Boric-Lubecke O, Lin J. A review on recent advances in Doppler radar sensors for noncontact healthcare monitoring. IEEE Transactions on microwave theory and techniques. 2013 May;61(5):2046-60.

[19] Nieh CM, Lin J. Adaptive beam-steering antenna for improved coverage of noncontact vital sign radar detection. In2014 IEEE MTT-S International Microwave Symposium (IMS2014) 2014 Jun 1 (pp. 1-3). IEEE.

[20] Bancroft R. Microstrip and printed antenna design. The Institution of Engineering and Technology; 2009.

[21] Rabbani MS, Ghafouri-Shiraz H. Improvement of microstrip patch antenna gain and bandwidth at 60 GHz and X bands for wireless applications. IET Microwaves, Antennas & Propagation. 2016 Apr 15.

[22] Rabbani MS, Ghafouri-Shiraz H. Improvement of microstrip antenna's gain, bandwidth and fabrication tolerance at terahertz frequency bands. InWideband and MultiBand Antennas and Arrays for Civil, Security & Military Applications 2015 Dec 2 (pp. 1-3). IET.

[23] Rabbani MS, Ghafouri□Shiraz H. Size improvement of rectangular microstrip patch antenna at MM□wave and terahertz frequencies. Microwave and Optical Technology Letters. 2015 Nov 1;57(11):2585-9.

[24] Li C, Lin J. Optimal carrier frequency of non-contact vital sign detectors. In2007 IEEE Radio and Wireless Symposium 2007 Jan 9 (pp. 281-284). IEEE.

[25] Rabbani MS, Ghafouri-Shiraz H. Ultra-Wide Patch Antenna Array Design at 60 GHz Band for Remote Vital Sign Monitoring with Doppler Radar Principle. Journal of Infrared, Millimeter, and Terahertz Waves. 2016:1-9.

[26] Obeid D, Sadek S, Zaharia G, El Zein G. Multitunable microwave system for touchless heartbeat detection and heart rate variability extraction. Microwave and optical technology letters. 2010 Jan 1;52(1):192-8.

[27] NHS. Online at: http://www.nhs.uk/chq/Pages/2024.aspx,

[28] Liu Y, Chen S, Ren Y, Cheng J, Liu QH. A broadband proximity-coupled dual-polarized microstrip antenna with L-shape backed cavity for X-band applications. AEU-International Journal of Electronics and Communications. 2015 Sep 30;69(9):1226-32.

[29] Zhang W, Li K, Jiang W. Micro-motion frequency estimation of radar targets with complicated translations. AEU-International Journal of Electronics and Communications. 2015 Jun 30;69(6):903-14.

[30] Kafshgari S, Mohseni R. Fluctuating target detection in presence of non Gaussian clutter in OFDM radars. AEU-International Journal of Electronics and Communications. 2013 Oct 31;67(10):885-93.